

REPORT DOCUMENTATION PAGE			Form Approved OMB NO. 0704-0188	
Public Reporting burden for this collection of information is estimated to average 1 hour per response, including the time for reviewing instructions, searching existing data sources, gathering and maintaining the data needed, and completing and reviewing the collection of information. Send comment regarding this burden estimates or any other aspect of this collection of information, including suggestions for reducing this burden, to Washington Headquarters Services, Directorate for information Operations and Reports, 1215 Jefferson Davis Highway, Suite 1204, Arlington, VA 22202-4302, and to the Office of Management and Budget, Paperwork Reduction Project (0704-0188,) Washington, DC 20503.				
1. AGENCY USE ONLY (Leave Blank)		2. REPORT DATE July 10, 2006		3. REPORT TYPE AND DATES COVERED Final Technical Report Jan 1, 2003-July 1, 2006
4. TITLE AND SUBTITLE Ceramics Containing Layers Designed for Increased Resistance to Fragmentation Damage <i>See Report</i>		5. FUNDING NUMBERS N00014-03-1-0350		
6. AUTHOR(S) Frederick F. Lange, PI				
7. PERFORMING ORGANIZATION NAME(S) AND ADDRESS(ES) Materials Department College of Engineering University of California Santa Barbara, CA 93106-5050		8. PERFORMING ORGANIZATION REPORT NUMBER NA		
9. SPONSORING / MONITORING AGENCY NAME(S) AND ADDRESS(ES) Office of Naval Research Ballston Centre Tower One 800 North Quincy Street Arlington, VA 22217-5660		10. SPONSORING / MONITORING AGENCY REPORT NUMBER		
11. SUPPLEMENTARY NOTES The views, opinions and/or findings contained in this report are those of the author(s) and should not be construed as an official Department of the Army position, policy or decision, unless so designated by other documentation.				
12 a. DISTRIBUTION / AVAILABILITY STATEMENT Approved for public release; distribution unlimited.		12 b. DISTRIBUTION CODE		
13. Abstract Stresses and Crack Extension in Multi-Layered Ceramic Composites  F. F. Lange Materials Department, University of California at Santa Barbara Santa Barbara, CA 93106 USA  It has been demonstrated, through theory and experiments, that compressive layers arrest large surface and internal cracks to produce a stress below which the material will not fail. This enables the materials to have a Threshold Strength. The stress intensity function, K, was derived for a crack sandwiched between two compressive layers. This function suggests that the threshold strength is proportional to the magnitude of the residual, compressive stress, the thickness of the compressive region, and inversely proportional to the distance between the compressive regions. All of these factors have been experimentally examined for laminar composites containing thin, compressive layers. Cracks that propagate straight through the layer obey the K function used to model this behavior. Crack bifurcation, which occurs at high compressive stresses, produces a larger threshold strength than predicted. Crack bifurcation is not fully understood.  During the initial studies, differential thermal contraction during cooling from the densification temperature was used to develop the compressive stresses. A molar volume change to induce the compressive stress was also used to develop the compressive stresses. In one case, it was shown that the compressive stresses could arise when the compressive layer contained a material that underwent a structural phase transformation during cooling. In another, ion exchanged glass plates that are subsequently bonded together also produce a threshold strength. Factors that affect the threshold strength are reviewed.				
14. SUBJECT TERMS Review, laminar, ceramics, composites, compressive stresses, threshold strength, bifurcation, edge-cracking, crack interaction			15. NUMBER OF PAGES 19	
17. SECURITY CLASSIFICATION OR REPORT UNCLASSIFIED			16. PRICE CODE	
18. SECURITY CLASSIFICATION ON THIS PAGE UNCLASSIFIED			20. LIMITATION OF ABSTRACT UL	
19. SECURITY CLASSIFICATION OF ABSTRACT UNCLASSIFIED				

NSN 7540-01-280-5500

Standard Form 298 (Rev.2-89)  
Prescribed by ANSI Std. Z39-18  
298-102

20060801349

# Stresses and Crack Extension in Multi-Layered Ceramic Composites

F. F. Lange

Materials Department, University of California at Santa Barbara  
Santa Barbara, CA 93106 USA  
flange@engineering.ucsb.edu

**Keywords:** laminar, ceramics, composites, compressive stresses, threshold strength, bifurcation, edge-cracking, crack interaction

**Abstract.** It has been demonstrated, through theory and experiments, that compressive layers arrest large surface and internal cracks to produce a stress below which the material will not fail. This enables the materials to have a Threshold Strength. The stress intensity function,  $K$ , was derived for a crack sandwiched between two compressive layers. This function suggests that the threshold strength is proportional to the magnitude of the residual, compressive stress, the thickness of the compressive region, and inversely proportional to the distance between the compressive regions. All of these factors have been experimentally examined for laminar composites containing thin, compressive layers. Cracks that propagate straight through the layer obey the  $K$  function used to model this behavior. Crack bifurcation, which occurs at high compressive stresses, produces a larger threshold strength than predicted. Crack bifurcation is not fully understood.

During the initial studies, differential thermal contraction during cooling from the densification temperature was used to develop the compressive stresses. A molar volume change to induce the compressive stress was also used to develop the compressive stresses. In one case, it was shown that the compressive stresses could arise when the compressive layer contained a material that underwent a structural phase transformation during cooling. In another, ion exchanged glass plates that are subsequently bonded together also produce a threshold strength. Factors that affect the threshold strength are reviewed.

## Introduction

The strength of a brittle material is not a singular value, but a distributed set of values that reflect the large variety of flaws (types and sizes) that are incorporated during processing. The distribution of strength values obtained during testing, all made at one time, are generally characterized by statistical parameters that vary with the processing method and processing period. That is, most manufacturers cannot control the nature of the flaws they inadvertently incorporate during processing. Proof testing, i.e., the application of a specific stress to a component, can be used to truncate the statistical distribution, to define a minimum, or threshold strength, for components that do not fail the proof test. Although there is a significant cost to proof testing, it allows the designer to ensure reliability.

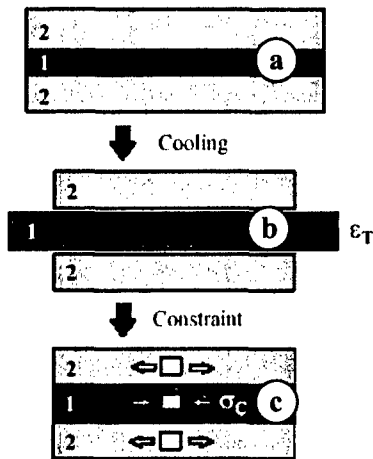
It was recently shown that a threshold strength (i.e., a strength below which the probability of failure is zero) can be obtained in laminar ceramics composed of periodic, alternating layers of one material separated by thinner layers of a second material. [1] The second layer must contain a residual, biaxial compressive stress produced by either differential thermal contraction or a molar volume change, e.g., a phase transformation. A threshold strength has been the 'holy grail' of structural ceramics. It has been demonstrated that large flaws within

the thicker layers that extend at a low stress will arrest as they entered the compressive layers. An increasing stress must be applied to 'push' the crack through the compressive layers to cause catastrophic failure. For periodic laminates, failure never occurs below a threshold stress despite large differences in the initial size of the crack present in the thicker layers.

Although this review will concentrate on laminates that can exhibit a threshold strength, the general background concerning stresses and crack extension in laminate composites will be reviewed first.

## Stresses in Multi-Layered Composites

**Bi-axial Stresses Deep within Layers.** Laminates formed at elevated temperatures with two or more materials develop stresses during cooling due to different thermal-elastic properties. For example, during cooling from  $T_0$  to  $T$ , the differential thermal contraction of one material sandwiched between two identical layers of a second material will produce a strain given by [2]



$$\epsilon_r = \int_T^{T_0} (\alpha_2 - \alpha_1) dT, \quad (1)$$

where  $\alpha_1$  and  $\alpha_2$  are the thermal expansion coefficients of the two materials.

Figure 1 helps to visualize how the internal residual stresses arise during cooling. Figure 1a shows the material with the lower thermal expansion coefficient sandwiched between the other material. When the layers are not bonded together, the two layers with the greater thermal expansion coefficient will contract more than the other during cooling as shown in Fig. 1b. If they were bonded together and cooled, both would contain the same strain at the lower temperature given by eq. (1). To determine the biaxial stresses in both

materials, one needs to apply biaxial compressive stresses to the layer(s) with the smaller thermal contraction such that the dimensions of all layers match one another. As the applied compressive stress is released after all are bonded together, all three layers will increase their length. During this step, residual stresses will arise in all three layers. These residual stresses will depend on the residual strain, given by eq. (1), the different elastic properties of the two materials and their respective volume fractions, which for a laminate, is given by the thickness ratio of the two materials.

To understand the effect of elastic properties, one can assume that the elastic modulus of the two sandwiching layers in Fig. 1 are either infinite or zero. When infinite, they will not expand, and the residual compressive stress within the center layer will not relax as the applied compressive stress is removed. When the elastic modulus of the outer layers is zero, the center layer will completely relax to its unconstrained dimensions as the applied compressive stress is removed; namely, no residual stresses will develop in any of the layers. The effect of the volume fraction of the two materials is easily understood by recognizing that the sum of the tensile and compressive forces ( $F_1$  and  $F_2$ ) acting across the respective cross sections ( $A_1$ ,  $A_2$ ) of the two materials must equal zero; namely, no resultant force exists to cause the laminate to move in the space-time coordinates. Thus, for a laminate shown in Fig. 1,

$$F_1 + F_2 = \sigma_1 A_1 + \sigma_2 A_2 = 0 \quad \text{or} \quad \sigma_2 A_2 = -\sigma_1 A_1 \quad (2)$$

Since all layers are assume to have the same width ( $w$ ), and  $A_i = t_i w$  ( $i = 1, 2$ ), then

$$\sigma_2 = -\sigma_1 \frac{t_1}{t_2}. \quad (3)$$

Along with eq. (3) it can be shown that the residual compressive (or tensile) stress that arises in this laminate can be expressed by [2]

$$\sigma_1 = \varepsilon_r E'_1 \left( 1 + \frac{t_1}{t_2} \frac{E'_1}{E'_2} \right)^{-1} \quad (4)$$

where  $E'_i = E_i/(1-\nu_i)$ ,  $E$  is the Young's modulus, and  $\nu$  is the Poisson's ratio.

Because crack extension initiates via tensile stresses, one generally attempts to fabricates a laminar composite to minimize the tensile stress. Assuming that the tensile stress ( $\sigma_t$ ) resides in material 2, eq. (3) shows that the tensile stress can be minimized by making the tensile layers thick relative to the compressive layers. Namely, the tensile stresses can be minimized when the tensile layers are much thicker than the compressive layers,  $t_2 \gg t_1$ . Thus, as  $t_1/t_2 \rightarrow 0$ ,  $\sigma_t \rightarrow 0$ . Like wise, the maximum compressive stresses ( $\sigma_c$ ) can be developed when  $t_1/t_2 \rightarrow 0$ , which from eq. (4) becomes

$$\sigma_c = \varepsilon_r E'_1. \quad (5)$$

The above summary assumes that the composite is symmetric, namely, the net stresses on one side of the center line are balanced by the net stresses on the other side, as shown in Fig. 1. Bending stresses would arise if the laminate was non-symmetric. Although the strain used above was assumed to arise due differential thermal expansion, molar volume changes due to a structural phase transformation and/or a chemical reaction (two phases that react to form a third phase) can produce the same state of stress.

**Tri-axial Stresses At and Near the Surface.** Although the biaxial stresses, described by Eqs. (3) and (4), exist deep within each layer, different stresses exist at and near the external surface. At the surface, the stresses are biaxial, and become tri-axial just below the surface.[2] Of most interest is the case for the layer that contains, biaxial compressive stresses far from the free surface. In this case, tensile stresses exist perpendicular to the center line at and near the surface as shown in Fig. 2 a.

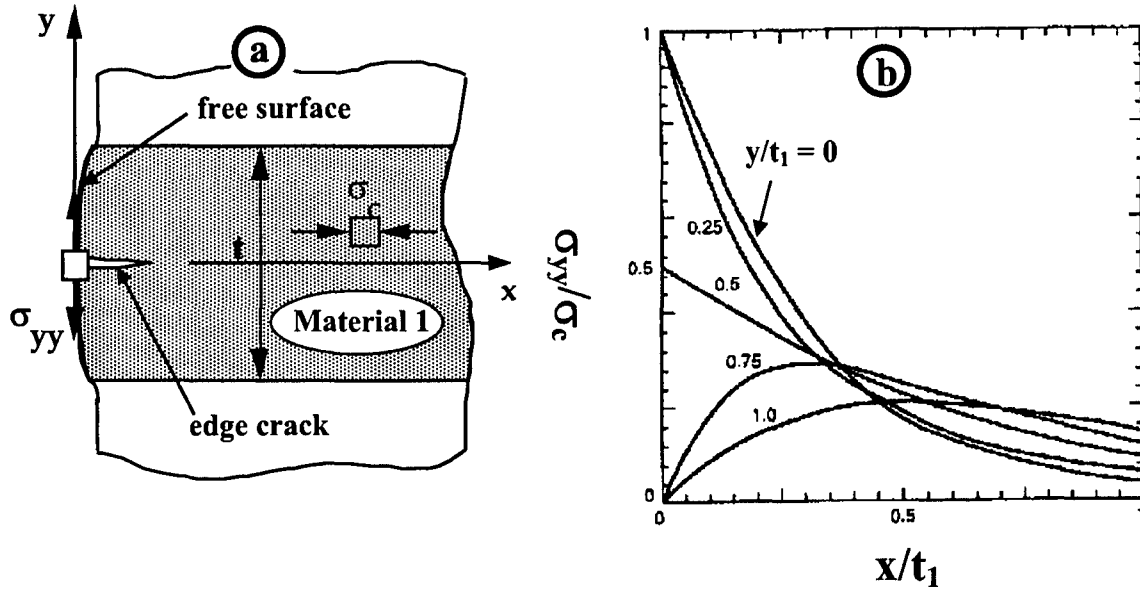


Figure 2 a) Schematic of the compressive layer terminating at a free surface and the associated tensile stress,  $\sigma_{yy}$  [2] that b) changes as a function of  $x$  and  $y$  as shown, when normalized by  $\sigma_c$ , the biaxial compressive stress far from the free surface.[3]

The largest tensile stress occurs at  $y = 0$ ; they are given by [2,3]

$$\sigma_{yy}(x)|_{y=0} = \frac{2}{\pi} \left[ \theta - \frac{1}{2} \sin 2\theta \right] \sigma_c \quad (6)$$

where  $x$  is the distance from the free surface,  $\tan \theta = t_1/2x$ , and  $\sigma_c$  is the absolute value of the residual biaxial compressive stress far from the free surface ( $x \gg 0$ ). As shown by Eq. (6), the tensile stresses have a maximum value at the surface ( $x = 0$ ) and diminish to a negligible value at a distance from the surface that is approximately equal to the thickness of the compressive layer.

Figure 2b shows [3] the distribution of the residual stress component  $\sigma_{yy}$  near the surface of a thin layer, assumed to be under biaxial compression far from the free surface. The centerline of the thin layer coincides with the  $x$ -axis ( $y = 0$ ). On the surface ( $x = 0$ ),  $\sigma_{yy}$  is a step-function, equal to  $|\sigma_c|$  in the thin layer,  $|\sigma_c|/2$  at the interface between the thin and thick layers, and zero in the two adjacent thick layers. Equation (6) is labeled as  $y/t = 0$  in Fig. 4. Figure 2b also illustrates  $\sigma_{yy}$  vs.  $x/t$  for other specific values of  $y/t$ . It can be shown that the other principle stresses close to the surface, namely,  $\sigma_{xx}$  and  $\sigma_{zz}$ , are compressive stresses. It can be shown that  $\sigma_{xx}(x) = \sigma_{yy}(x) + \sigma_c$ , and  $\sigma_{zz} = \sigma_c$ , thus,  $\sigma_{xx}(0) = 0$  and  $\sigma_{xx} \rightarrow \sigma_c$  as  $x \rightarrow t$ .

Of less interest are the tri-axial stresses at the free surface that terminates a layer containing biaxial tensile stresses  $\sigma_t$  deep within the layer. For this case, it can be shown [3] that  $\sigma_{yy}(x)$  is similar to eq. (6), except that  $\sigma_t$  is substituted for  $\sigma_c$ ; namely, a compressive stress exists where the tensile layer terminates at a free surface.

## Crack Extension in Brittle Laminates

**Edge-Cracking due to Tri-Axial State of Stress.** It has also been shown that because the tensile stresses are highly localized near the surface of the compressive layer, they can give rise to a surface crack, called an edge crack. The edge crack extends along the center line of the compressive layer when either the layer thickness and/or the value of compressive stress exceeds a critical value. The determination of the strain energy release rate function for edge-cracking is very similar to other problems associated with highly localized states of stress. These problems include the formation of microcracks around inclusions, cracking of thin films, crack extension associated with Hertzian contact stresses, and tunnel cracking in the tensile layer of laminar composites that will be discussed below. With the exception of cracking associated with the localized, Hertzian contact stresses, all of these problems are associated with a residual state of stress and the fact that crack extension reduces the stored strain energy within a localized volume of material.

For the current problem, i.e., the formation of an edge crack, the tensile stress is localized within the compressive layer in a region where the layer terminates at a free surface. With the assumption that the compressive layer is very thin compared to the two adjacent tensile layers (Fig. 1), only the stresses associated with compressive layer need be considered, namely, the stresses within the tensile layers are very small. The strain energy release rate function for the edge crack can be derived using a dimensional analysis by further assuming that the laminate is cylindrical, with a radius  $R$ . Prior to the formation of an edge crack, the total strain energy within the compressive layer can be defined as  $U_{sc}^0$ . When a small crack is able to extend to form an edge crack that circumvents the compressive layer, the strain energy associated with the compressive layer containing the edge crack is reduced and can be expressed as

$$U_{sc} = U_{sc}^0 - \left( \frac{F \sigma_c^2}{E^*} \right) (2\pi R Z c t_1), \quad (7)$$

where  $t$  is the thickness of the compressive layer,  $\sigma_c$  is the compressive stress deep within the layer,  $c$  is the length of the crack that extends from the surface into the compressive layer,  $2\pi R Z c t_1$  is the volume associated with the circumferential surface crack in which the strain energy has been released, and  $Z$  is a dimensionless constant that helps defines this volume. The factor  $\left( \frac{F \sigma_c^2}{E^*} \right)$  is the strain energy per unit volume in the compressive layer, close to the free surface,  $F$  is a dimensionless function that relates the stresses,  $\sigma_{yy}(x)$  and  $\sigma_{xx}(x)$  to  $\sigma_c$ .

The energy consumed during crack extension is given by

$$U_s = 2\pi R c G_c, \quad (8)$$

where  $4\pi R c$  is the area of the circumferential surface crack, and  $G_c$  is the critical strain energy release rate for the material that forms the compressive layer.

Summing eqs. (7) and (8), the total free energy as a function of the crack length is given by

$$U_t = U_{sc}^0 - \left( \frac{F \sigma_c^2}{E^*} \right) (2\pi R Z c t_1) + 2\pi R c G_c. \quad (9)$$

An examination of eq. (9) shows that the free energy of the system will only decrease when the sum of the second and third terms is negative, namely, when

$$\left(\frac{F\sigma_c^2}{E^*}\right)(2\pi R Z c t_1) > 2\pi R c G_c \text{ or } Z t_1 \left(\frac{F\sigma_c^2}{E^*}\right) > G_c \quad (10)$$

Thus it can be concluded that for fixed values of  $\sigma_c$ ,  $G_c$  and  $E^*$ , the edge crack will only form when

$$t_1 > t_c = \frac{G_c E^*}{Z F \sigma_c^2}, \quad (11)$$

where  $t_c$  is the critical layer thickness to produce an edge crack. The reason for this is that for given values of  $\sigma_c$ ,  $G_c$  and  $E^*$ , the highly localized strain energy, which depends on the thickness of the compressive layer, is only sufficient to compensate for the work needed to produce a crack when  $t_1 \geq t_c$ . A rigorous analysis of this problem shows that the numerical constants  $ZF = 0.34$ . [2]

**Tunnel Cracking in the Tensile Layer [4].** In this section, crack extension in the layers containing biaxial tensile stresses will be detailed; these layers will be called 'tensile layers'. If

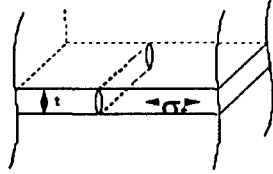


Figure 3 Schematic of a tunnel crack within a tensile layer, terminating at a free surface. [4]

the residual tensile stress is large enough, it will cause pre-existing flaws to "tunnel" through the layer to terminate at the free surface that bound the layer as shown in Fig. 3. Under biaxial tension, multiple tunnel cracks produce a 'mud' crack pattern, similar to those seen in thin films.

Consider a crack of length 'a' in a tensile layer of thickness t constrained and sandwiched by much thicker layers, such that the biaxial compressive stress in the thicker layers is assumed to be zero. It will be assumed that both materials have identical elastic properties and identical critical strain energy release rates,  $G_c$ . We assume that the crack can extend across the interface into the adjacent compressive layers and continue its extension as a tunnel crack shown in Fig 3. The strain energy release rate function for a slit crack,  $G_s$ , within a layer subjected to tension and bounded by adjacent layers that contain no stress can be found in Tada, et. al. [5], and given by

$$G_s = \left(\frac{\pi}{2}\right) \frac{\sigma^2}{E_1^*} \left(\frac{a}{t}\right) t, \quad a < t \quad (12)$$

and

$$G_s = \left(\frac{2}{\pi}\right) \frac{\sigma^2}{E_1^*} \left(\frac{a}{t}\right) \left(\sin^{-1}\left(\frac{t}{a}\right)\right)^2 t, \quad a > t \quad (13)$$

where  $E_1^* = E_1/(1-\nu_1^2)$ ,  $E_1$  and  $\nu_1$  are the Young's modulus and Poisson's ratio of the tensile layer. Figure 5 plots  $G$  normalized by  $\frac{\sigma^2 t}{E_1^*}$  as a function of the normalized crack length,  $a/t$ . As

the slit length 'a' increases, the energy release rate increases when the slit is within the tensile layer,  $a/t < 1$ , and sharply decays when the slit extends into the adjacent thicker layers,  $a/t > 1$ .

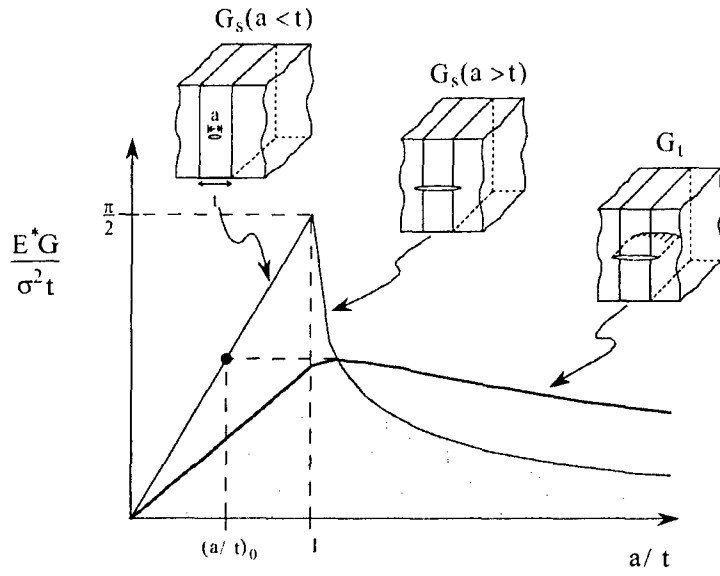


Figure 4 Plot of the normalized strain energy release rate for crack extension ( $G_s$ ) and crack tunneling ( $G_t$ ) versus normalized crack length ( $a/t$ ). When  $(a/t)$  is greater than  $(a/t)_0$ , crack extension occurs without tunneling. Further cooling (equivalent to increasing the residual stress) is required to initiate crack tunneling. When  $(a/t)$  is less than  $(a/t)_0$ , crack extension occurs with tunneling [4]

layer is  $(a/t)_s \leq a/t \leq 1$  (see Fig. 4), then, during cooling the horizontal line will intersect the hatched region and the crack will extend without tunneling to a normalized size that is slightly larger than  $a/t = 1$ . Further cooling will cause the horizontal line to enter the hatched field for  $G_t$  such that the slit crack will tunnel through the tensile layer. On the other hand, if the normalized size of the initial slit crack is  $0 < (a/t)_s$ , the horizontal line will first enter the hatched area where the initial slit crack will both extend to become  $a/t > 1$  and tunnel at the same time.

Figure 4 can also be used to interpret crack extension for the case where the laminate contains tensile layers of different thicknesses that has been cooled to room temperature, thus fixing the tensile stress in all of the layers to the same value. By viewing Fig. 4, it can be seen that the initial slit crack cannot tunnel, regardless of its initial size, if the horizontal line of the normalized fracture energy,  $\frac{G_c E_1^*}{\sigma^2 t}$ , is above the maximum point on the  $G_t$  curve, which is  $\pi/2$ .

Rearrange it can be shown [4] that one obtains a critical thickness for the tensile layer for which no pre-existing crack, regardless of its size, can tunnel. The critical layer thickness is given by

$$t_c = \left( \frac{2}{\pi} \right) \frac{G_c E_1^*}{\sigma^2} \quad (14)$$

When  $t \geq t_c$  the probability of tunneling will still depend on the size of the flaw that pre-exists within the tensile layer.

The above analysis assumes identical elastic properties and identical fracture energy for both materials. When the adjacent layers are more compliant than the tensile layer (smaller

$G_t$  was determined numerically [4]; it is plotted in Fig. 4. The strain energy release rate for tunneling,  $G_t$ , is small where the width of the crack, 'a' is both small and large; it reaches the maximum value when it slightly extends into the adjacent layers. This maximum point coincides with the intersection of the  $G_s$  and  $G_t$  functions.

Knowing the critical strain energy release rate,  $G_c$ , the elastic modulus  $E^*$ , the tensile stress in the layer  $\sigma$ , and the layer thickness  $t$ , one can use Fig. 4 as a 'map' to determine the conditions for when the crack will extend across the tensile layer and tunnel along its length.. The value of the

normalized fracture energy,  $\frac{G_c E_1^*}{\sigma^2 t}$ , can

be represented by a horizontal line in Fig. 4. During cooling, the line moves down because the residual tensile stress increases. Assuming the normalized size of the largest crack in the tensile

elastic modulus), the normalized energy release rate increases and the slit crack will extend a greater distance into the adjacent layers. The opposite condition occur when the tensile layer is more compliant then the adjacent material.

**Crack Bifurcation Under Bending Loads [6,7].** Once it was discovered that edge cracking would occur, as reviewed above, another phenomenon associated with laminar materials was investigated, leading to the discovery that laminates exhibiting edge cracking would also exhibit

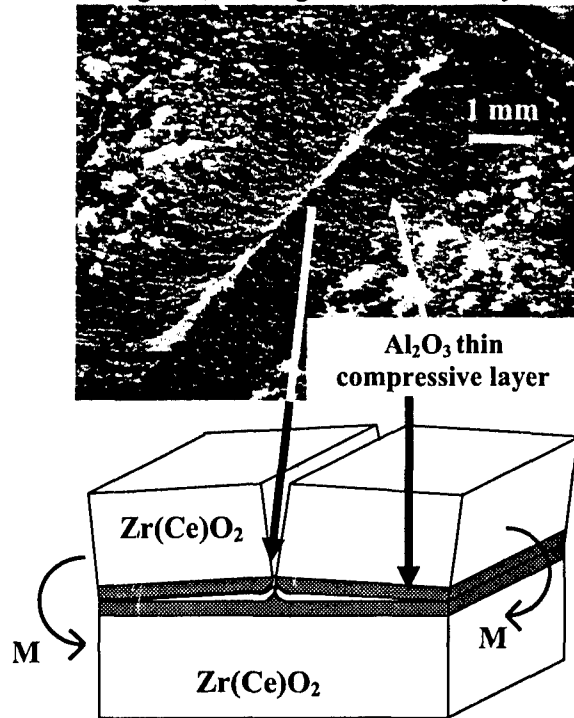


Figure 5 At bottom, illustration of an crack extending into a compressive layer and bifurcating to continue its extension along the center line of the compressive layer under a bending moment,  $M$ . Micrograph shows the fracture surface where the white areas are the  $ZrO_2$  and the dark,  $Al_2O_3$ . [6]

a new phenomenon where cracks that would extend into a compressive layer would bifurcate. The observations associated with bifurcation in the compressive layer under bending loads will be reviewed in this section. Bifurcation under tensile loads will be reviewed in a subsequent section.

The thinking that lead to experiments concerning crack bifurcation were based on the following ideas. When a crack propagates through a material, it obviously creates a free surface. When it approaches the compressive layer, the crack will create a new free surface that will terminate the different layers within the composite. A tensile stress similar to that described by eq. (6) will arise due to the introduction of the free surface. It was reasoned that since the stress in front of the crack would be converted from a compressive stress acting perpendicular to the crack plane to a tensile stress acting parallel to the crack plane, the crack path might be altered to produce a bifurcated crack. It was also expected that the conditions required for bifurcation would be similar to the conditions for edge cracking, namely, bifurcation would be expected to occur when  $\sigma_{yy}t_1 > \text{critical value}$ , where  $\sigma_{yy}$  is the tensile stress (eq.6), and  $t_1$  is the thickness of the compressive layer.

To test this idea, flexural loading experiments were conducted using specimens fabricated from two different material systems, namely composites formed with  $Zr(Ce)O_2$  thick layers and  $Al_2O_3$  thin, compressive layer, [6] and composites formed with  $Al_2O_3$  thick layers and mullite/ $Al_2O_3$  [7] thin, compressive layers. Figure 5 illustrates the bending moment relative to the layers. For both composite systems it was demonstrate that during fracture, cracks extending perpendicular to the compressive layer would bifurcate and extend along the centerline of the compressive layer. In addition, bifurcation should only occur if the specimen also contained an edge crack prior to fracture. Namely, the conditions for edge cracking and bifurcation were similar, i.e.,  $\sigma_{yy}t_1 > \text{critical value}$ . Figure 5 illustrates this bifurcation phenomenon. For the specimen shown in Fig. 5, the crack begins to bifurcate prior to entering the compressive layer. Because the two materials have a different atomic number, i.e., the  $Zr(Ce)O_2$  scatters more electrons and thus appears white, relative to the darker  $Al_2O_3$  compressive layer, the white ridge on top of the 'mountain' created by the bifurcation clearly shows that bifurcation starts within the  $Zr(Ce)O_2$  layer. The micrograph also

shows that the crack 'dives' down to a plane near the lower interface between the two materials (white regions) and then rises to propagate close to the center line of the  $\text{Zr}(\text{Ce})\text{O}_2$  compressive layer (not shown).

The experiments also showed that when bifurcation occurred, the extending crack did not continue through the composite. If the loading was stopped, the specimen could be retrieved before it fully fractured. If the loading was continued, crack extension would only occur with the extension of a new crack at some location along the compressive layer. Bifurcation would occur each time the crack entered a new compressive layer, and further crack extension would only continue when a new crack would reinitiate the failure sequence. This failure phenomena produce a much higher strain to failure relative to a composite that did not exhibit crack bifurcation.

Bifurcation during tensile loading, which is related to the threshold strength that special laminar composites can exhibit, will be discussed below.

### **Architectural Design of Layered Composites that Produce a Threshold Strength**

**Need for a Threshold Strength.** The strength of brittle materials, including ceramics and glasses, must be described by statistical parameters (e.g. Weibull) because they contain an unknown variety of cracks and crack-like flaws inadvertently introduced during processing and surface machining. Proof testing must be used when performance outweighs consumer price sensitivity. The proof test is designed to emulate the thermal/mechanical stresses experienced by the component in severe service. The proof test defines a threshold stress below which components are eliminated by failure prior to service. Eliminating heterogeneities from the ceramic powder that give rise to flaws is another method to ensure reliability. One method to remove inclusions and agglomerates greater than a given size is to disperse the powder in a liquid and pass the slurry through a filter.[8] Providing heterogeneities are not reintroduced in subsequent processing steps and surface cracks introduced during machining are not a critical issue, filtration determines a threshold strength by defining the largest flaw that can be present in the powder, and thus, within the finished ceramic component. Methods for forming engineering shapes with filtered slurries have been developed.[9]

Although others [10-13] have shown that residual, compressive surface stresses will hinder the growth of surface cracks, Green et al. [14] have proposed that the compressive stress should be located a specific distance beneath the surface. By doing so, they suggest the compressive stress will better arrest surface cracks, leading to higher failure stresses and reduced strength variability. However, compressive stresses, either at or just beneath the surface, will not effectively hinder internal cracks and flaws, nor can they produce a threshold strength. As shown below, a threshold strength can only arise when thin compressive layers are placed throughout the body to interact with both surface cracks and internal cracks/flaws.

The hypothesis that multiple, thin compressive layers could lead to a threshold strength had its genesis in an observation made by a co-worker (Sánchez-Herencia) when a crack was observed to initiate and arrest between two compressive layers during experiments to further understand the phenomena associated with crack bifurcation.[6,7] This observation initiated a fracture mechanics analysis to determine the conditions for crack arrest and subsequent failure, and experiments to test the analysis.[1]

The analysis assumed that a pre-existing crack of length  $2a$  spans the thick layer ( $t_2$ ), sandwiched by the compressive, thin layers of thickness  $t_1$ . The biaxial, residual compressive stress within the thin layers is given by  $\sigma_c$ , while the opposing residual tensile stress within the thick layer is given by  $\sigma_t$ . The analysis determines the stress intensity factor for a crack of length

2a when it extends into the compressive layers ( $t_2 \leq 2a \leq t_2 + 2t_1$ ), under an applied stress,  $\sigma_a$ , parallel to the layers. The stress intensity factor is used to determine the applied stress,  $\sigma_{thr}$ , needed to extend the crack through the compressive layers to produce catastrophic failure.

**Stress Intensity Function for Crack Extension Through the Compressive Layer [1].** The stress intensity function,  $K$ , is determined by superimposing two stress fields, each applied to the same crack, and each with a known stress intensity factor. Using the rules of super-positioning, the stress intensity factors for each of the stress fields are then summed to determine the stress intensity factor for the crack that extends into the compressive layers. The first stress field is a tensile stress ( $\sigma_a - \sigma_c$ ) applied to the whole specimen; its stress intensity factor is given by the first term in eq. (2a). The second is a tensile stress of magnitude ( $\sigma_c - \sigma_t$ ), applied only across the portion of the crack that spans the thicker layer,  $t_2$ ; its stress intensity factor is given by the second term in eq. (2a).[1]

$$K = (\sigma_a - \sigma_c) \sqrt{\pi a} + (\sigma_c - \sigma_t) \sqrt{\pi a} \left[ \frac{2}{\pi} \sin^{-1} \left( \frac{t_2}{2a} \right) \right] \quad (15)$$

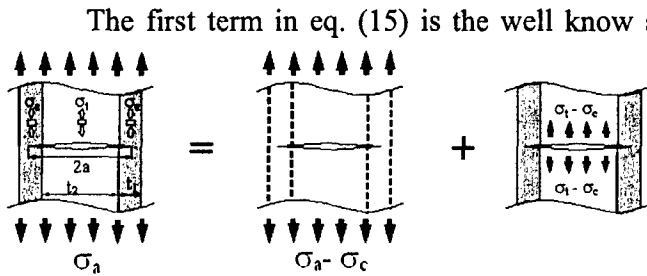


Figure 6. Crack of length 2a shown penetrating two, bounding compressive layers placed under an applied stress  $\sigma_a$ . The stress state on the left can be split into the two superimposed stress states on the right.

The first term in eq. (15) is the well known stress intensity factor for a slit crack in an applied tensile field. The second term is always negative and thus reduces the stress intensity factor when the crack enters the compressive layers. Thus, the compressive layers increase the material's resistance to crack extension.

Since  $K$  decreases as the crack extends into the compressive layers, the maximum stress needed to cause the crack to 'break' through the compressive layers occurs when  $2a = t_2 + 2t_1$  and  $K = K_c$ , the critical stress intensity factor

of the thin layer material, a property that describes its intrinsic resistance to crack extension. Substituting these values into eq. (15) and rearranging, the largest stress needed to extend the crack through the compressive layers is given by

$$\sigma_{thr} = \frac{K_c}{\sqrt{\pi \frac{t_2}{2} \left( 1 + \frac{2t_1}{t_2} \right)}} + \sigma_c \left[ 1 - \left( 1 + \frac{t_1}{t_2} \right) \frac{2}{\pi} \sin^{-1} \left( \frac{1}{1 + \frac{2t_1}{t_2}} \right) \right] \quad (16)$$

Equation (16) shows that  $\sigma_{thr}$  increases with the fracture toughness of the thin layer material,  $K_c$ , the magnitude of the compressive stress,  $\sigma_c$ , and the thickness of the compressive layer,  $t_1$ . One can also show that if the initial crack length in the thick layer is  $< t_2$ , and the stress needed to extend it is  $< \sigma_{thr}$ , the crack will be arrested by the compressive layers. On the other hand, if the crack is very small and extends at a stress  $> \sigma_{thr}$ , it will extend through the compressive layers to cause catastrophic failure without being arrested. Thus, eq. (16) defines a

threshold stress,  $\sigma_{thr}$ , below which the laminar body cannot fail when the tensile stress is applied parallel to the layers.

**Threshold Strength: Experimental Findings [15,16]** Equation (16) was confirmed by using both Finite Element Analysis (FEA) [17] and an experimental method where the stable extension



Figure 7 Micrographs of acetate replicas for a crack extending straight through a compressive layer (defined by broken lines) with increasing applied stress. As shown in Fig. 3, the length of crack as a function of stress was used to confirm the  $K$  expression given in eq(15). [15]

of the crack was sequentially observed to extend through the compressive layer with increasing applied load. The FEA also showed that the threshold strength would increase as the ratio of the elastic modulus of the thin, compressive layer material to the thicker, tensile layer material was decreased. Namely, the strain energy density is smaller in a compressive layer with a smaller elastic modulus.

Because the crack extends in a stable manner, it can be directly observed as it sequentially propagates across the compressive layer with

increasing applied stress. Figure 7 shows a crack that was replicated, in situ, with acetate tape at different stresses as it extended across the compressive layer with increasing applied stress. [15] The shadowed replica was then observed with an optical microscope using Nomarski interference. The stress intensity function can be experimentally determined by plotting the crack length vs. applied stress. These measurements confirm the theoretical  $K$  function given by Eq. (15). [15]

Equation (15) shows that an increasing stress is needed to extend the crack through the compressive layers, which implies a new toughening mechanism. From an engineering standpoint, eq. (15) can be rearranged to state a more important concept, i.e., a threshold exists, below which, failure is impossible. The applied stress needed to fully extend the crack through the compressive layer is called the threshold strength,  $\sigma_{th}$ . Failure occurs once the crack fully extends through the compressive layer (i.e. when  $2a = t_2 + 2t_1$ ) and  $K \geq K_c$ .

Observations show that the crack does not always propagate straight across the compressive layers as implied by eq. (15). Instead, when either the compressive stress or the thickness of the compressive layer is large, the crack bifurcates as two cracks as it traverses the compressive layer. On the other hand, when the compressive stress and/or compressive layer thickness is small, the crack does not bifurcate. Namely, when a edge crack is observed in the compressive layers before testing, the crack that extends across the interface exhibits bifurcation. This suggests that similar phenomena produce both edge cracking and crack bifurcation both in bending modes of loading as discussed above, and also in tensile modes of loading as discussed here.

Figure 8 shows that the crack bifurcates either within or as it enters the compressive layer of laminates with the 55 $\mu$ m/550 $\mu$ m architecture. [16] The figure also shows that the angle between the two cracks changes from 115° to 122° to 135° with increasing compressive stress for compressive layers containing 0.40, 0.55 and 0.70 volume fraction mullite, respectively. It should be noted that in addition to the bifurcated crack, except for the region between the bifurcated cracks a linear crack is also observed along the centerline of the compressive layer. [16]

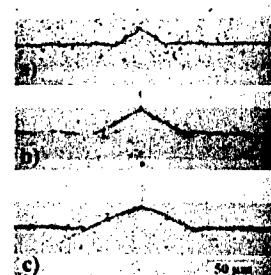


Figure 8 Crack bifurcation in compressive layers with increasing compressive stress (a to c). [16]

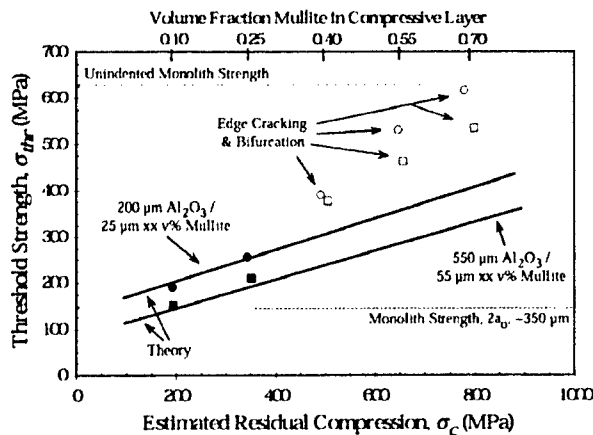


Figure 9. Effect of compressive stress on threshold strength measure for laminates with two different architectures (laminates dimensions). [16]

mullite content) while also fixing the  $t_1/t_2$  ratio. The residual compressive stresses within the thin compressive layers of some representative architectures were measured using a piezospectroscopic method which determines stress by measuring the stress-induced shift in the fluorescence spectra of trace  $\text{Cr}^{3+}$  impurities within the alumina. [18]

The results of these studies can be generalized in Fig. 9, which shows the effect of the compressive stress on the threshold strength for two different architectures, one with  $t_1/t_2 = 25 \mu\text{m}/200 \mu\text{m}$  and the other with  $t_1/t_2 = 55 \mu\text{m}/550 \mu\text{m}$ . The results could be divided into two regimes. [16] In the first regime, in which the compressive stress was  $< 400 \text{ MPa}$ , the threshold strengths for the two architectures agreed well with those predicted by eq. 16. For this regime, the crack propagated straight through the compressive layer as shown in Fig. 7. On the other hand, for compressive stresses  $> 400 \text{ MPa}$ , the experimental values of the threshold strength were progressively greater than those predicted by eq. 16. For this second regime, the crack was observed to bifurcate through the compressive layer as shown in Fig. 8.

The bifurcated cracks shown in Fig. 8 were observed after removing the surface by diamond matching to a depth below the penetration depth of the original edge crack. [16] The edge cracking observed in Fig. 8 is an artifact which extended as the new free surface was exposed by grinding, as is evidenced by its absence between the branches of the bifurcated crack where the tensile surface stresses were relieved by bifurcation.

Hbaieb et al [19] have investigated the bifurcation phenomenon via a finite element analysis based on the material properties for laminar composites studied by Rao and Lange [16] (Fig. 9). The strain energy release rates for the straight and bifurcated cracks were calculated from the results of finite element computations and compared. When the stresses due to edge cracking were ignored, the crack was simulated as a through-thickness crack in an infinite body, and the energy release rate was used to predict crack deviation and bifurcation by comparing the magnitude of the strain energy release rate function for the two cases. Namely, bifurcation would only be favored and expected if the magnitude of the strain energy release rate function,  $G$ , was greater than that for the straight through crack. The finite element model successfully predicts bifurcation in only one of the four composites that were experimentally studied. When the stress field, and thus strain energy of the edge cracking was incorporated into the finite element simulations, the strain energy release rate calculations successfully predict the phenomenon of bifurcation in three of the four composites, as observed in the experiments. The presence of edge cracking, was concluded to be important to the occurrence of crack bifurcation in laminar ceramic composites.

Several of the variables can be easily changed to determine their effect on the threshold strength. For these studies, laminar composites composed of thicker alumina layers separated by thinner alumina/mullite layers were fabricated. One of the variables, the compressive stress, was systematically changed by changing the volume fraction of the mullite, to reduce thermal expansion, in the thinner alumina/mullite compressive layers for fixed  $t_1/t_2$  ratios. [16] A second variable, the distance between the compressive layers,  $t_2$ , was changed by fabricating different laminates with different values of  $t_1$  at a fixed compressive stress (i.e., fixed

**Strength of Laminar Composites with Thin, Porous Layers [20].** As discussed above, a finite element analysis showed that a laminar composite could have a much larger threshold strength if the compressive layers had a much smaller elastic modulus relative to the thicker, tensile layers. [19] The reason for this is because the compressive layer would have a smaller strain energy density, reducing the applied stress intensity factor within the compressive layer. This condition would require a higher applied stress to drive the crack through the compressive layer. Thus, for a crack to extend across the compressive layer and cause failure, the applied stress must be sequentially increased to counteract the "shielding" effects of both the residual compressive stress and modulus mismatch. It was estimated that the influence of the elastic modulus mismatch could be significant.

In order to study the effects of elastic modulus mismatch, porosity was introduced into the thin compressive layers via adding pore-forming agents such as starch particles. One composite contained thick  $\text{Al}_2\text{O}_3$  layers and thin layers composed of a mixture of  $\text{Al}_2\text{O}_3$  and 0.50 or 0.70 volume fraction of mullite (designated 50M and 70M) used to control the magnitude of the compressive stress, and rice starch particles to introduce the porosity. Rice starch readily disperses in aqueous solutions, and is easily removed from a powder compact by pyrolysis. In a second composite system, the thick layers were also formed with  $\text{Al}_2\text{O}_3$ . The thin layers in the second composite system contained unstabilized zirconia (MZ- $\text{ZrO}_2$ ) mixed with  $\text{Al}_2\text{O}_3$  plus the rice starch to produce the porosity. These composites were designated 20MZ and 50MZ. In this case, the  $\text{ZrO}_2$  would undergo a tetragonal to monoclinic structural phase transformation during cooling and also produce a large density of microcracks as detailed elsewhere.[21] The compressive stresses were measured by the piezospectroscopy technique pioneered by Clarke and his students [18].

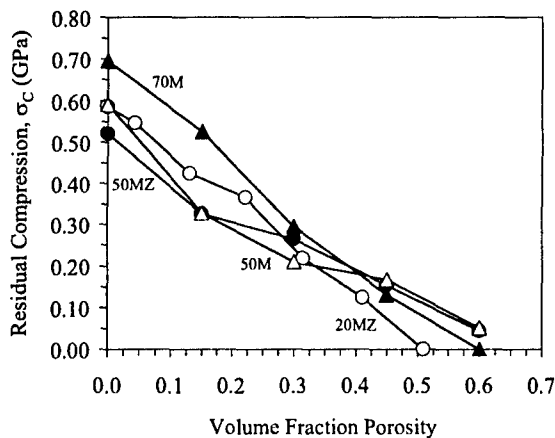


Figure 10 Values of the compressive stresses produced in the thin ( $t_1$ ) porous layers by laminar constraint, as determined by piezospectroscopic analysis of the thick ( $t_2$ ) layers. Open and closed triangular symbols denote results for the 50M and 70M laminates, while the open and closed circular symbols denote results for the 20MZ and 50MZ laminates, respectively. [20]

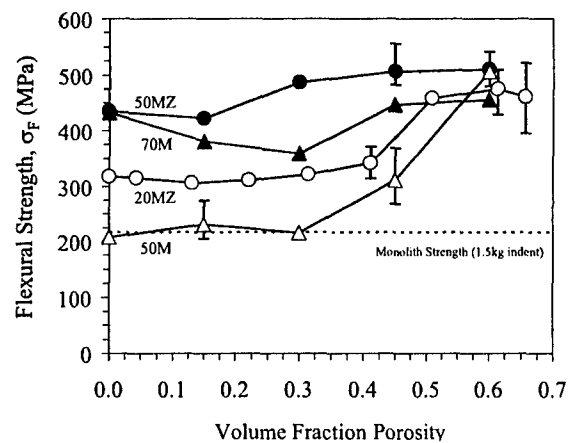


Figure 11 Four-point bending flexural strength versus volume fraction of porosity in the thin compressive layers, for laminate specimens containing a single 1.5 kg Vickers indent. Open and closed triangular symbols denote results for the 50M and 70M laminates, while the open and closed circular symbols denote results for the 20MZ and 50MZ laminates, respectively. The dashed line indicates the strength of an  $\text{Al}_2\text{O}_3$  monolith containing the same size indent. [20]

It was shown that as the volume fraction of porosity was increased, the residual compressive stress ( $\sigma_c$ ), elastic modulus ( $E_1$ ), and critical stress intensity factor ( $K_{Ic}$ ) of the thin layers were reduced, approaching zero at approximately 0.65 volume fraction of porosity. Figure

10 shows the residual compressive stress as a function of the porosity introduced into the thin layers. Despite the large reduction in  $\sigma_c$  and  $K_c$ , Fig. 11 shows that the flexural strength did not significantly change with increasing volume fractions of porosity, and actually increased as the volume fraction of porosity in the thin compressive layers was  $> 0.40$ . These specimens exhibited a different mode of fracture relative to other laminates studied by the Lange Group at UCSB; namely, a crack propagating across any one of the thick layers was completely arrested by the thin, porous layers, and did not continue into an adjacent thick layer as shown by a number of fractured thick layers in Fig. 12. Micrographs of these highly porous layers showed that they are not able to support a continuous crack front. That is, fracture in these highly porous layers would have to occur by the sequential fracture of one supporting polycrystalline ligament after another. However, it appeared that cracks in adjacent thick layers would initiate, extend, and stop before ligaments failed within the porous layers. This occurrence would not be unreasonable since a stress singularity would be associated with any pre-existing crack in dense, thick layer, whereas the 'cracks' within the porous layer do not have a stress singularity. Alternately, since the elastic modulus of the thin, porous layers  $\rightarrow 0$ , the strain energy that drives the crack through the porous layers also  $\rightarrow 0$ . Thus it appeared that crack extension across each laminate was determined by the statistical distribution of flaws throughout all the dense laminate layers. Eventually, after a number of layers failed, catastrophic failure of the laminate occurs by shear failure (delamination) of the porous layers. Specimens failing in this manner did not exhibit a threshold strength; namely, crack extension in any one of the dense, thick layers was governed by the statistical distribution of cracks in each thick layer.

Both types of mechanical behavior, i.e., the inhibited extension of a crack across a compressive layer and the complete arrest of a crack due to sufficient porosity, are very promising for structural ceramics in general. As shown above, decreasing the elastic modulus of thin compressive layers within a body increases the energy required to drive a crack through the structure, resulting in a greater threshold strength. Additionally, by creating interlayers with volume fractions of porosity within a critical range, the integrity of the ceramic body can be maintained, while cracks within the body are completely arrested. Failure of the body, due to linking of the flaws within separate layers, can be controlled by reducing the number of inherent flaws produced in the body during fabrication or subsequent machining. In addition, during the sequential failure of one thick layer after another, the load-displacement behavior exhibits an extended strain to failure shown in Fig. 13, which in itself is a useful phenomenon.

### Interaction of Cracks in Laminates that Exhibit a Threshold Strength [22]

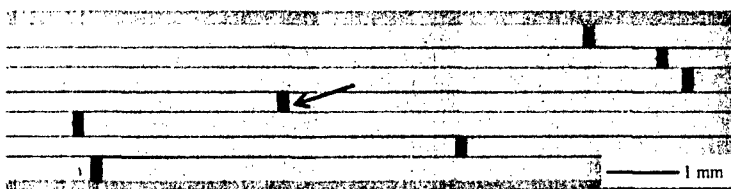


Figure 12 Optical micrograph showing the fracture pattern on the tensile surface of a 20MZ laminate specimen with thin compressive layers containing 0.61 volume fraction porosity. The arrow denotes the location of a 1.5 kg Vickers indent used to initiate failure during 4-point bending. The thick layers broke randomly and were eventually linked by cracking or delamination within the porous layers. [20]

Although a single crack within a thick, tensile layer can be successfully arrested by the thin compressive layers, there is a finite probability that large cracks can exist close to one another in adjacent thick layers. Several researchers have used different methods to obtain solutions for the stress intensity factor of interacting cracks. It was shown that the two closely spaced cracks can interact to increase the stresses at the

outer ends of the two cracks.[23] In photoelastic studies of two closely spaced cracks, it was shown that two cracks tend to act as one large crack once they overlap, and coalescence does not occur until they overlap.[24]

The purpose of this section is to review the experimental findings concerning the interaction of cracks in adjacent thick layers, separated by thin compressive layers. As shown in Fig. 14 cracks were systematically introduced at the surface of the thick layers with an indenter and the strength of these specimens was measured as a function of their off-set, separation distance,  $x$ . As discussed below, the crack-crack interaction reduced the threshold strength of the laminar ceramic in a predictable way. It is also shown that the position of the crack affected the threshold strength as well.

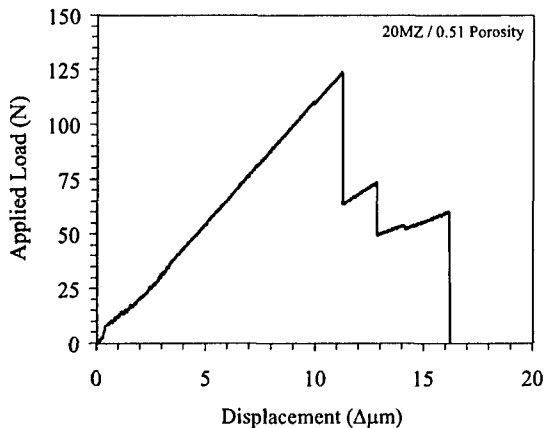


Figure 13 Load-displacement plot for a 20MZ laminate specimen with thin compressive layers containing 0.51 volume fraction porosity. The specimen, containing a single Vickers indent of 1.5 kg, was tested in 4-point bending until complete failure. [20]

Four different laminate architectures were fabricated. For each, the threshold strength for non-interactive cracks is (labeled 'Single Crack' in Fig. 14). The off-set distances ( $x$ ) between two cracks were normalized with respect to  $t_2$ , the thickness of the thick, tensile layer. Figure 14 shows the strength of specimens containing two off-set cracks, normalized by the strength of a single crack versus the normalized off-set separation distance ( $x/t_2$ ) for the four laminates. Each point represents the strength of one specimen from one of the four different laminates. As shown, the strength of double indented specimens depends on the off-set separation distance. The largest decrease in normalized strength was 0.72, and occurred when the normalized, off-set separation distance was 0, i.e., for two co-planar cracks. The strength of the double indented specimens was  $< 1$  until the

normalized off-set separation distance was  $\geq 2$ .

Figure 14 shows the crack paths for interacting of two typical cracks. All evidence suggests

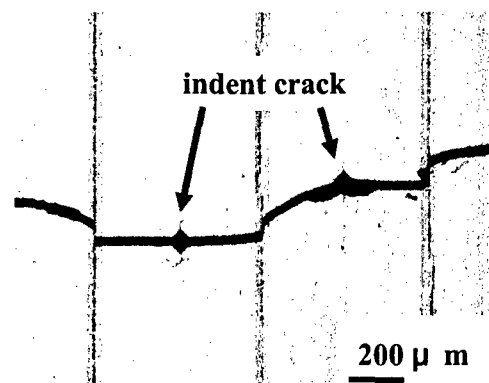
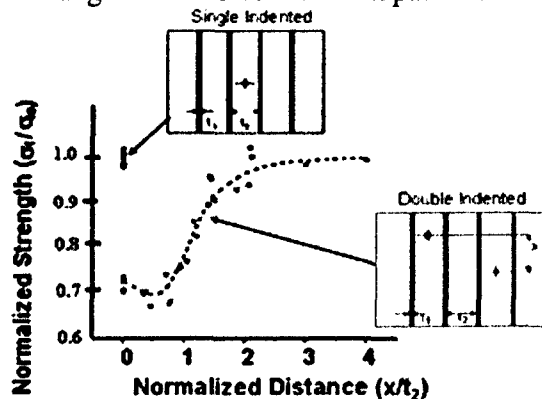


Figure 14 Reduction of threshold strength when two cracks are introduced into adjacent thick layers, separated by an off-set distance,  $x$ . Micrograph show that the two adjacent cracks share a common crack path when the separation distance is small. [22]

that the two indentation cracks extended across their thick layers, and at some load, coalesced after breaking through their separating, compressive layer. The cracks extended though the two outer

compressive layers at a prescribed stress that, as discussed below, can be predicted with knowledge of the distance between the outer, compressive layers.

As shown in Fig. 14, the strength decreased with increasing off-set separation distance for normalized, off-set separation distances between 0 and 0.5. Within this range, the two cracks coalesced as shown in Fig. 14. For a normalized off-set separation distance of 1.4 (not shown) the two cracks did not coalesce, yet these specimens did exhibit a reduction in threshold strength as reported in Fig. 14. As the normalized off-set separation distance is increased further, the interaction between the two cracks diminishes such that the normalized strength recovers to 1 when the normalized, off-set separation distance ( $x/t_2$ ) is between 2 and 3.

Moussa et al. [23] reported the finite element results of two parallel, semi-elliptical, surface cracks with different lateral and off-set separations ( $x = 0.3, 0.5$  and  $1.0$ ). They showed that when the off-set separation distance was  $> 2$ , each crack behaved as if isolated from one another. As the off-set separation distance decreased to zero, the stress intensity factor of the inter-crack tips increased relative to that for an isolated crack of the same length and applied stress. This increase was greater for smaller values of the off-set separation. When the normalized, lateral separation distance became  $< 0$  (two cracks overlap one another), the stress intensity factor of the inner crack tip was smaller relative to the isolated crack, and larger for the outer crack tips. That is, for substantial overlap, the two smaller cracks would act as one larger crack. The magnitude of the increased stress intensity factor at the inner crack tips before overlap, and the increased stress intensity factor for the outer cracks tips after overlap diminished with increasing normalized, off-set distance ( $x$ ). In addition, the inner crack tips exhibited an increasing Mode II stress intensity factor, suggesting that the paths of the inner crack tips would change, one, or the other, seeking to extend towards its neighboring crack as suggested by the photoelastic study of Lange [23].

Observations for two cracks, separated by a single compressive layer, are consistent with the finite element (FE) studies summarized above [23]. The FE results suggested that the initial cracks, introduced by indentation, would not interact with one another because their lateral separation distance was too large. If this were the case, they would only begin to interact at the critical applied stress that would cause them to extend across their respective, thicker, tensile layers. Observations, such as the one shown in Fig. 14 indicates that their separating compressive layer did stop the cracks before they further extended to coalesce as predicted by the FE studies.

Equation 16 suggests that when  $t_1/t_2$  is small, as for specimens prepared for the crack interaction study, the threshold strength will be inversely proportional to the square root of the dimension of the thicker layer,  $t_2$ . Thus, if one were to double the dimension of the thick layer, the normalized value of the threshold strength should be 0.71 relative to a non-interacting crack within one thick layer. As shown in Fig. 14, for normalized off-set values  $< 1$ , the normalized threshold strength is approximately 0.7; this data shows that when the off-set value produces strongly interactive cracks, the threshold strength is reduced by the inverse square root of the number of interacting cracks within adjacent thick layers.

## Concluding Remarks

As reviewed above, a threshold strength can be achieved in laminar composites containing thin, compressive layers. But this concept has limitation as implied by the study of interacting cracks. Namely, when the thick layers become approximately the same dimension as the inherent crack size within these layers, there will be an increased probability that cracks within the thick layers will interact such that the concept of a threshold strength will no longer have any meaning. Thus, the concept explored here to produce a threshold strength is only valid when the dimensions of the thick layers are much larger than the size of the inherent cracks within these layer. Further, it was shown that thin layers containing large amounts of porosity could stop cracks, and that the cracks in one

thick layer did not progress through to the next thick layer. The implications of this observation requires further study.

### Acknowledgements

The author is grateful for the support of the Office of Naval Research via contract Grant: N00014-03-1-0350 and to Steven G. Fishman for his generous support of my research career. The author thanks all the students, Matthias Oechsner, Craig Hillman, Kais Hbaieb, Michael Pontin, Hak-Sung Moon, Geoff Fair and Mark Snyder that took part in this work and Javi Sánchez-Herencia for his initial observations leading to the discovery of the Threshold Strength phenomenon. The author also thanks his UCSB colleagues, Bob McMeeking and Glenn Beltz for their significant contributions to what they called 'baby' fracture mechanics, and to Zhigang Suo, now at Harvard.

### References

- [1] M. P. Rao, A. J. Sánchez-Herencia, G. E. Beltz, R. M. McMeeking and F. F. Lange, *Science*, 286, pp 102-5, Oct. 1 (1999).
- [2] S. Ho, C. Hillman, F.F. Lange and Z. Suo, *J. Am. Ceram. Soc.* 78 [9] 2353-59 (1995).
- [3] A.J. Monkowski AJ and G. E. Beltz, *Inter. J. Solids and Structures*, 42 [2] 581 (2005).
- [4] C. Hillman, Z. Suo, and F.F. Lange, *J. Am. Ceram. Soc.* 79 [8] 2127-2133 (1996).
- [5] H. Tada, P. C. Paris, and G. R. Irwin, *The Stress Analysis of Cracks Handbook*, 2nd ed., Del Research, St. Louis, MO, 1985.
- [6] M. Oechsner, C. Hillman, and F.F. Lange, *J. Am. Ceram. Soc.* 79 [7] 1834-38 (1996).
- [7] A. J. Sanchez-Herencia, C. Pascual, J. He, F.F. Lange, *J. Am. Ceram. Soc.*, 82 [6] 1512-1518 (1999).
- [8] F. F. Lange, *J. Am. Ceram. Soc.* 72 [1] 3-15 (1989).
- [9] B.C. Yu and F.F. Lange, *Advanced Materials*, 13, No. 4, 2001.
- [10] P. Honeyman-Colvin and F. F. Lange, *J. Amer. Ceram. Soc.* 79 [7], 1810 (1996).
- [11] F. F. Lange and B. I. Davis, *J. Am. Ceram. Soc.* 62 [11-12], 629 (1979).
- [12] D. J. Green, *J. Mater. Sci.* 19 [7], 2165 (1984).
- [13] R. Lakshminarayanan, D. K. Shetty, R.A. Cutler, *J. Am. Ceram. Soc.* 79 [1], 79 (1996).
- [14] D. J. Green, R. Tandon, V. M. Sglavo, *Science* 283, 1295 (1999).
- [15] M. P. Rao, J. Rödel, and F. F. Lange, *J. Am. Ceram. Soc.*, 84, 2722-24 (2001).
- [16] M. P. Rao and F.F. Lange, *J. Am. Ceram. Soc.* 85 [5] 1222-8 (2002).
- [17] K. Hbaieb and R. M. McMeeking, *Mech. Mat.* 34 [12] 755-72 (2002)
- [18] Q. Ma and D. R. Clarke, *J. Am. Ceram. Soc.* 77 [2] 298-302 (1994).
- [19] K. Hbaieb, R.M. McMeeking and F. F. Lange, to be published.
- [20] M.G. Pontin and F.F. Lange, *J. Am. Ceram. Soc.*, 88 [2] 376-382 (2005).
- [21] M.G. Pontin, M.P. Rao, A.J. Sánchez-Herencia and F.F. Lange, *J. Am. Ceram. Soc.*, 85 (12) 3041-48 (2002).
- [22] H. Moon, M.G. Pontin, F.F. Lange, *J. Am. Ceram. Soc.* 87 [9] 1694-1700 (2004)
- [23] W. A. Moussa, R. Bell, and C. L. Tan, *Int. J. Press. Vessels Piping*, 76 [3] 135-45 (1999).
- [24] F. F. Lange, *Int. J. Fracture Mech.* 4 [9] 287-94 (1968).